



ELSEVIER

Journal of Alloys and Compounds 323–324 (2001) 584–591

Journal of  
ALLOYS  
AND COMPOUNDS

www.elsevier.com/locate/jallcom

# Some recent developments in the characterization of ceria-based catalysts

Alessandro Trovarelli\*, Marta Boaro, Eliana Rocchini, Carla de Leitenburg, Giuliano Dolcetti

*Dipartimento di Scienze e Tecnologie Chimiche, Università di Udine, Via Cotonificio 108, 33100 Udine, Italy*

## Abstract

In the present paper some recent developments in the use of ceria and related materials in catalysis are considered. The relevant features of ceria–zirconia and ceria–silica as oxygen storage components are briefly reviewed with a special focus on the characterization and relationship between oxygen uptake/release and structural properties. © 2001 Elsevier Science B.V. All rights reserved.

*Keywords:* Ceria; Ceria–zirconia; Ceria–silica; Oxygen storage; Diffusion; CeO<sub>2</sub>

## 1. Introduction

Rare-earth oxides have been widely investigated as structural and electronic promoters to improve the activity, selectivity and thermal stability of catalysts. The most significant of the oxides of rare-earth elements in industrial catalysis is certainly CeO<sub>2</sub> [1]. Its use in catalysis has attracted considerable attention in recent years, especially for those applications, such as treatment of emissions, where ceria has shown great potential [2].

There are also several emerging applications or processes for which cerium oxide is currently being actively investigated. Specifically, CeO<sub>2</sub> has potential uses for the removal of soot from diesel engine exhaust, for the removal of organics from wastewaters (catalytic wet oxidation), as an additive for combustion catalysts and processes, and in redox reactions [1]. In addition to these applications, much effort has been dedicated recently to studying the role of ceria in well-established industrial processes such as fluid catalytic cracking and three-way-catalysts, where CeO<sub>2</sub> is a key component in catalyst formulation [3].

The success of ceria and CeO<sub>2</sub>-based materials is mainly due to the unique combination of an elevated oxygen transport capacity coupled with the ability to shift easily between reduced and oxidized states (i.e. Ce<sup>3+</sup>–Ce<sup>4+</sup>). These properties are strongly dependent on the structural features of the specific catalyst formulation used (atomic and phase composition), and further development of the

materials concerned will therefore require more detailed information on their chemistry in the solid state. For example the role of different components and phase composition, the kinetics of the O<sub>2</sub> uptake/release and the influence of the preparation procedure on the above properties will have to be understood at a fundamental level in order to design advanced materials for emission treatment applications.

As a contribution to this area, we have been investigating for the last few years a number of issues concerning the synthesis and characterization of ceria-containing materials with regard to their application as redox and oxidation catalysts [4,5]. In this paper, we will briefly present some recent progress in this field based on results from our laboratory as well as from other institutions which are developing a new generation of ceria-based catalysts with special focus on the characterization of materials.

## 2. The role of ceria as an oxygen storage component

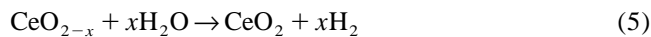
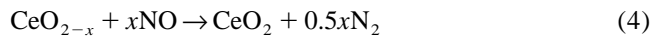
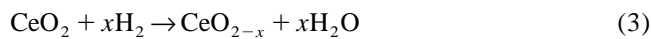
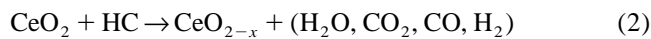
The most important commercial application of ceria in catalysis is certainly the treatment of exhaust gases from spark-ignited internal combustion engines. It is not the intent of this review to describe the utilization of ceria in auto exhaust catalysis as a number of papers have recently been published on the role of ceria in this technology [3,6,7], and only a brief summary of the main features of ceria will be given.

The catalyst formulation for auto exhaust treatment consists primarily of noble metals and metal oxides dispersed either on the surface of alumina pellets or on an

\*Corresponding author. Tel.: +39-0432-558855; fax: +39-0432-558803.

E-mail address: trovarelli@dstc.uniud.it (A. Trovarelli).

alumina washcoat anchored to a monolithic ceramic substrate. It is very well-known that the main role of ceria in this complex mixture is to provide oxygen buffering capacity during the rich/lean oscillation of exhaust gases. Under working conditions, the catalyst is in fact exposed to constantly varying feedstream compositions going alternately from rich exhaust stoichiometry (deficient  $O_2$ ) to lean stoichiometry (excess  $O_2$ ). In this environment, ceria has the ability to donate its oxygen for the removal of CO and hydrocarbons (HC) during the oxygen-deficient portion of the cycle (reactions (1)–(3)) while adsorbing and storing oxygen from  $O_2$ , NO and water during excursion into the lean part of the cycle (reactions (4)–(6)). These reactions positively affect the conversion of the three major pollutants (CO, HC and NO) under conditions typically encountered in the normal operation of a three-way catalyst.



If the atmospheric environment in which  $CeO_2$  operates changes continuously from a net oxidizing to a net reducing composition, the oxidation state of cerium correspondingly shifts from +4 to +3, enhancing the conversion of CO and hydrocarbons during rich oscillations, and of NO during lean oscillations. This unique feature of ceria is called oxygen storage capacity (OSC). It derives from the ability of  $CeO_2$  to be *easily* and *reversibly* reduced to several  $CeO_{2-x}$  stoichiometries when exposed to  $O_2$ -deficient atmospheres [8,9]. Removal of oxygen from ceria at high temperatures in fact leads to the formation of a continuum of O-deficient nonstoichiometric compositions of the type  $CeO_{2-x}$  ( $\alpha$  phase  $0 < x < 0.178$ ), as evidenced in the relevant state diagram [9]. Even after loss of oxygen from its lattice and the consequent formation of a large number of oxygen vacancies,  $CeO_2$  retains its fluorite crystal structure. This also facilitates rapid and complete refilling of oxygen vacancies upon exposure of  $CeO_{2-x}$  to oxygen, with recovery of  $CeO_2$ .

The major drawbacks of an oxygen storage system based on pure ceria is related to thermal resistance and low-temperature activity [10]. The main reason why  $CeO_2$  alone is of comparatively little interest as a support or catalyst is its textural stability, which is not high enough to meet the requirements of high-temperature gas-phase catalytic reactions. The surface area of  $CeO_2$  generally

drops to a few square meters per gram at around 1000–1100 K, depending on preparation procedure and type of treatment [11,12]. Another factor which discourages the use of pure ceria is its cost, which is higher than that of more common supports like  $Al_2O_3$  and  $SiO_2$ . Much effort has therefore been directed in recent years to finding catalyst formulations which can enhance the thermal stability of ceria without diminishing its special features, such as its redox properties and its high oxygen mobility. The main catalyst formulations studied contain either ceria spread over a thermally stable support like  $CeO_2$  deposited on  $Al_2O_3$  [13] or ceria thoroughly mixed with other oxides in mixed-oxides formulations or better in solid solutions [6]. New catalyst composition involves the use of ceria doped with other rare-earth or transition metal oxides. In this case the kinetics of oxygen transport is heavily modified and more efficient redox processes are permitted at much lower temperatures. Noble metals can also be used to improve catalyst activity.

### 3. The design of ceria-based mixed oxides as oxygen storage components

The excellent oxygen storage behavior of ceria is the result of a unique and delicate balance between structural (phase formation) kinetic (rate of redox of  $Ce^{4+/3+}$ ) and textural (presence of surface cerium sites) factors. For the design of  $CeO_2$ -based materials with high oxygen storage/transport capacity, it is therefore important to know the mechanism by which ceria can store, transport and release oxygen. According to the mechanism and dynamics of oxygen storage, an increase in the number and mobility of oxygen vacancies should lead to a corresponding increase in the ability of the material to take up and release oxygen. Therefore any chemical modification of  $CeO_2$  involving an increase in the number of structural defects (oxygen vacancies) should produce a material with a higher oxygen storage capacity. This is true providing that the chemical modification does not significantly reduce the number of active redox elements. In principle there are two ways in which we can operate to accomplish this. The first is to promote ceria reduction [14], and the second is to chemically dope ceria with other transition or rare-earth elements [15]. Promotion of ceria reduction can be accomplished either by noble metal deposition or by chemically modifying ceria with one or more dopant [16].

The choice of the dopant elements, and of the amounts to be employed, is a key factor in the design of modified ceria. The ability to substitute one cation for another in a particular structure is dependent on several factors, such as the dimensions of the host/guest cation and the structural features of the pure oxide [17], although the preparation method can also have a strong influence on the stability and homogeneity of a solid solution.  $CeO_2$  can easily form solid solutions with other rare earth elements and with

transition metals. Of the rare earth elements, Pr and Tb are particularly suitable for making solid solutions with cerium [18–22]. The known structure of  $\text{PrO}_2$  and  $\text{TbO}_2$  is of the cubic fluorite type and the ionic radii of  $\text{Pr}^{4+}$  and  $\text{Tb}^{4+}$  are close to that of  $\text{Ce}^{4+}$  [23].

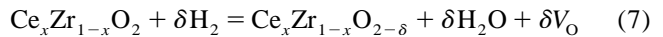
Regarding transition metals,  $\text{CeO}_2$  can form solid solutions with  $\text{ZrO}_2$  [24],  $\text{PbO}_2$  [25],  $\text{CuO}$  [26],  $\text{MnO}_x$  [27], although the range of stability and phase composition varies widely over these ions. With  $\text{Cu}^{2+}$  and  $\text{Mn}^{3,4+}$ , which have a lower ionic radius, solid solutions that retain the fluorite structure are formed only in a limited compositional range. Conversely, although the ionic radius of  $\text{Zr}^{4+}$  (0.84 Å) is smaller than that of  $\text{Ce}^{4+}$  (0.97 Å),  $\text{CeO}_2$  and  $\text{ZrO}_2$  form solid solutions quite easily and in a large composition range. Indeed, the use of  $\text{Zr}^{4+}$  as a dopant promotes the kinetics of  $\text{Ce}^{4+}$  reduction and enhances oxygen storage of ceria [6].

The formation of mixed oxides or better solid solutions does not represent the only way to improve the properties of ceria. We have recently shown that incorporation of small amounts of silica in a mixed ceria–silica composite is an effective way to increase the thermal behavior and the oxygen handling properties. In these conditions silicon is not dissolved within ceria lattice, but it forms separate  $\text{SiO}_2$  aggregates, which help keeping ceria crystallites small enough to guarantee an elevated oxygen exchange [28]. Below we will highlight some features of these systems.

#### 4. The $\text{CeO}_2$ – $\text{ZrO}_2$ system

Ceria–zirconia is one of the main components of current new generation of three-way catalysts (TWC) for the treatment of noxious pollutants from car exhaust [6]. It has gradually replaced pure cerium oxide ( $\text{CeO}_2$ ) whose characteristics were not adequate to sustain the high degree of conversion and the thermal resistance required for catalytic converters to meet the more severe regulations in terms of emissions of CO,  $\text{NO}_x$  and hydrocarbons. It has been used in the formulations of car exhaust catalysts since the early 1990s and this is evidenced by an almost exponential increase in the number of publications devoted to the catalytic features of this system in the last few years, following the first publications in the open literature in 1993 [29,30]. The main features which contribute to the success of ceria–zirconia are: (i) a higher thermal resistance if compared with conventional  $\text{CeO}_2$ -containing TWC, (ii) a higher reduction efficiency of the redox couple  $\text{Ce}^{4+}$ – $\text{Ce}^{3+}$ , and (iii) a good oxygen storage/release capacity. These features bring to an overall higher degree of conversion especially at low temperature, during start up, where the majority of emissions are produced. Most of the recent literature on this topic has focused on the study of the redox properties, related to the oxygen storage capacity (OSC) [4,6,14,31–36], although other catalytic applications were also investigated [37–40].

By monitoring the reduction of  $\text{CeO}_2$  in ceria–zirconia solid solutions according to reaction (7)



it is shown that the value of  $\delta$  varies with composition ( $x$  in Reaction (7)) and is almost independent on surface area (Fig. 1). The promotion of reduction is attributed to the enhanced oxygen mobility of solid solutions compared to the pure oxides [14]. However, the total degree of reduction is a parameter which is better related to the amount of oxygen which is thermodynamically available at a given temperature, that is generally called *total oxygen storage capacity*. The amount of oxygen transferred in a pulsed regime (following sequential reactions of the material with oxidizing and reducing mixtures), better simulates the oscillations that the exhaust gas may undergo during real operation and therefore is much more useful in the evaluation of specific activity of the material. This is therefore the oxygen which is kinetically available during the fast transitions between reduction and oxidation environments. It is a more important value than total  $\text{H}_2/\text{O}_2$  uptake since a large uptake is of no consequence unless it is reversible on the time-scale of exhaust fluctuations. For that reason, the actual importance of the process during dynamic operations is determined first by the rate of variations of oxygen content and second by the oxygen capacity of the material. By considering only fast exchangeable oxygen, results indicate that solid solutions with intermediate composition have the largest capacity of storing and releasing  $\text{O}_2$ . As an example Fig. 2 shows the behavior of Ce–Zr solid solutions in donating oxygen for CO oxidation under dynamic/pulse mode [41].

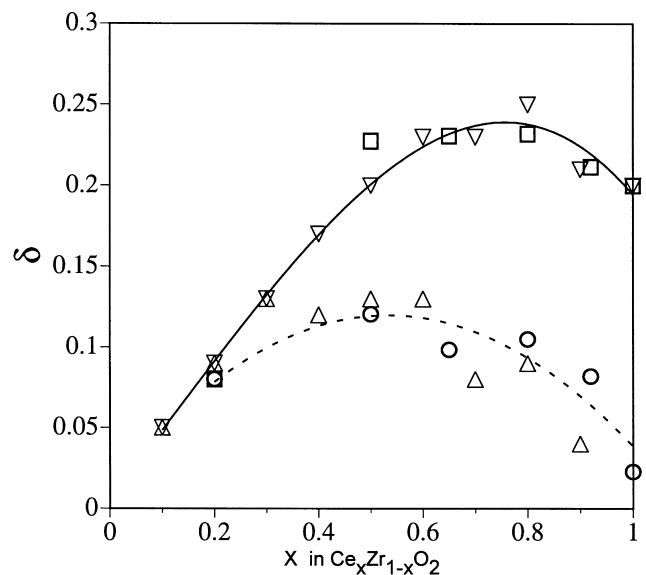


Fig. 1. Reduction extent of  $\text{Ce}_x\text{Zr}_{1-x}\text{O}_2$  to  $\text{Ce}_x\text{Zr}_{1-x}\text{O}_{2-\delta}$  after treatment under TPR conditions (5%  $\text{H}_2$  in Ar) at low (700–900 K, dotted line) and high temperature (1300 K, solid line): ( $\Delta$ ,  $\nabla$ ), low surface area samples [14] and ( $\square$ ) high surface area samples [38].

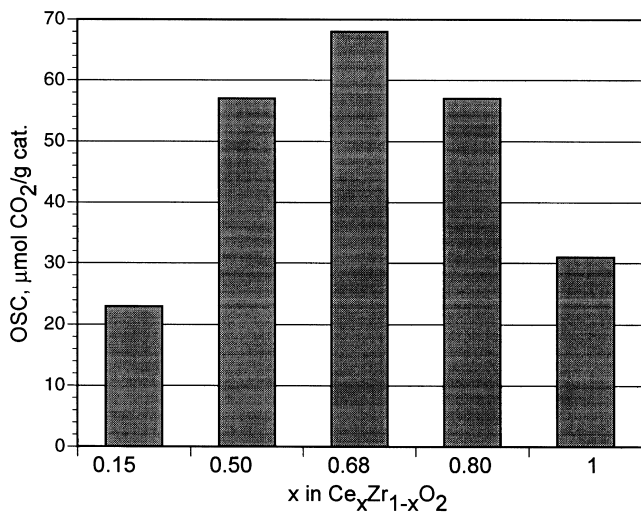


Fig. 2. Oxygen-storage capacity measured in pulse conditions for various Ce/Zr mixed oxides. Values measured after first pulse at 673 K [41].

Both steady state and transient results seem to indicate that optimum composition is around 50% of each oxide i.e. Ce<sub>0.5</sub>Zr<sub>0.5</sub>O<sub>2</sub>. The reason for this might be related to a delicate balance between number of redox centers (Ce atoms) and structural features. The formation of solid solutions with different structures in the CeO<sub>2</sub>–ZrO<sub>2</sub> system is mainly regulated by the methodology employed for preparation, and by composition (i.e. Ce/Zr ratio), although the exact nature of the phase diagram and transformation dynamics is still a matter of debate [6]. Generally, for CeO<sub>2</sub> contents lower than 10 mol%, monoclinic symmetry is preferred but for CeO<sub>2</sub> contents higher than 80 mol%, the phase diagram shows a monophasic region of cubic symmetry [24]. In the intermediate region, the exact nature of the phases is still unclear, because of the stable and metastable phases of tetragonal symmetry present. Yashima reported the formation of three different tetragonal phases, named *t*, *t'* and *t''* [42]: the *t* is a stable phase formed through high-temperature diffusional phase decomposition; the *t'* form is obtained through a diffusionless transition and is metastable with axial ratio  $c/a_f > 1$ ; and the *t''* form is also metastable but with  $c/a_f = 1$  [43]. This is a slight modification of a cubic structure and originates by oxygen anion displacement from an ideal fluorite site retaining  $c/a = 1$  (Fig. 3).

Several methods have been employed to prepare ceria–zirconia like coprecipitation starting from cerium and zirconium salts [44], sol–gel synthesis [45], template-assisted methods [46], microemulsion [47] and chemical filing processes [48]. We have recently reported that also high-energy mechanical milling (MM) is an effective method for the preparation of ceria–zirconia mixed oxides with a good degree of homogeneity over almost the entire composition range [49]. In this case X-ray diffraction studies pointed out the formation of a cubic solid solution for CeO<sub>2</sub>-rich samples (Ce<sub>x</sub>Zr<sub>1-x</sub>O<sub>2</sub>, with  $x > 0.5$ ), and an increasing degree of tetragonality for higher ZrO<sub>2</sub> loading.

Since it has been reported that solid solutions having a cubic cell have better oxygen storage properties than those with tetragonal symmetry [15], we have more deeply investigated the nature of phases formed. However, owing to the difficulty of detection of oxygens by XRD because of the lower scattering of O in comparison to Ce or Zr, powder neutron diffraction has been used to fully characterize the structural features of these materials [50].

The ‘state of the art’ phase diagram for this system is the one reported by Yashima et al. [24]. The tetragonal region starts at a composition of Ce<sub>x</sub>Zr<sub>1-x</sub>O<sub>2</sub> with  $x < 0.8$  with the pseudocubic *t''* phase. The stability of this phase spans a region of Ce<sub>x</sub>Zr<sub>1-x</sub>O<sub>2</sub> composition from  $0.65 < x < 0.8$ . Other authors have reported that the formation of *t''* phase extends beyond this region up to compositions with  $x = 0.5$  [51]. It is therefore clear that, due to the metastable nature of the phases formed, transition from one structure to the other may also be critically influenced by particle dimensions, and therefore by the methodology used for preparation [52]. In our case, the low temperature used in the synthesis (local increase of temperature may reach a few hundred degrees), and the continuous bond rupture/formation typical of mechanical milling, produced a material having a higher surface area with a particle size in the range of 100–170 Å. This could explain the stabilization of the *t''* phase even at a lower Ce content. The formation of this phase is characterized by the shift of oxygen atoms from their ideal position in an ordered fashion, which induces a distorted oxygen sublattice. The coordinate of oxygen was calculated at  $z_O = 0.04$  cell units (corresponding to an oxygen displacement of 0.21 cell units if compared to the position of oxygens in ceria where  $z_O$  is 0.25). A comparison with the only quantitative data existing in the literature on such oxygen shift in ceria–zirconia (for CZ50,  $z_O = \text{ca. } 0.21$ , corresponding to an oxygen displacement of ca. 0.17 Å) [53,54] indicates a higher degree of distortion in our samples, which may be indicative of the type of preparation and/or the higher surface area of our sample. This anion lattice distortion, in conjunction with the axial ratio value  $c/a_f = 1$ , indicates that the phase is closely related to a cubic cell, with a large shift of oxygens from their ideal positions. This may explain why the introduction of Zr into the CeO<sub>2</sub> lattice is beneficial to catalytic activity up to compositions close to Ce<sub>x</sub>Zr<sub>1-x</sub>O<sub>2</sub> with  $x = 0.5$ , where optimal activity is observed. The benefit could be the result of the high oxygen transport properties typical of the fluorite lattice, coupled with the presence of structural defects (like oxygen distortions) which enhance diffusion of oxygens. A quantitative estimate of the contribution of bulk diffusion to the overall performance (calculated from the diffusion coefficient for ceria–zirconia solid solutions obtained from conductivity measurements [55] using the Nernst–Einstein relation) shows that in the temperature range investigated bulk diffusion is approximately two orders of magnitude higher for ceria–zirconia than for ceria (Fig. 4), and it is

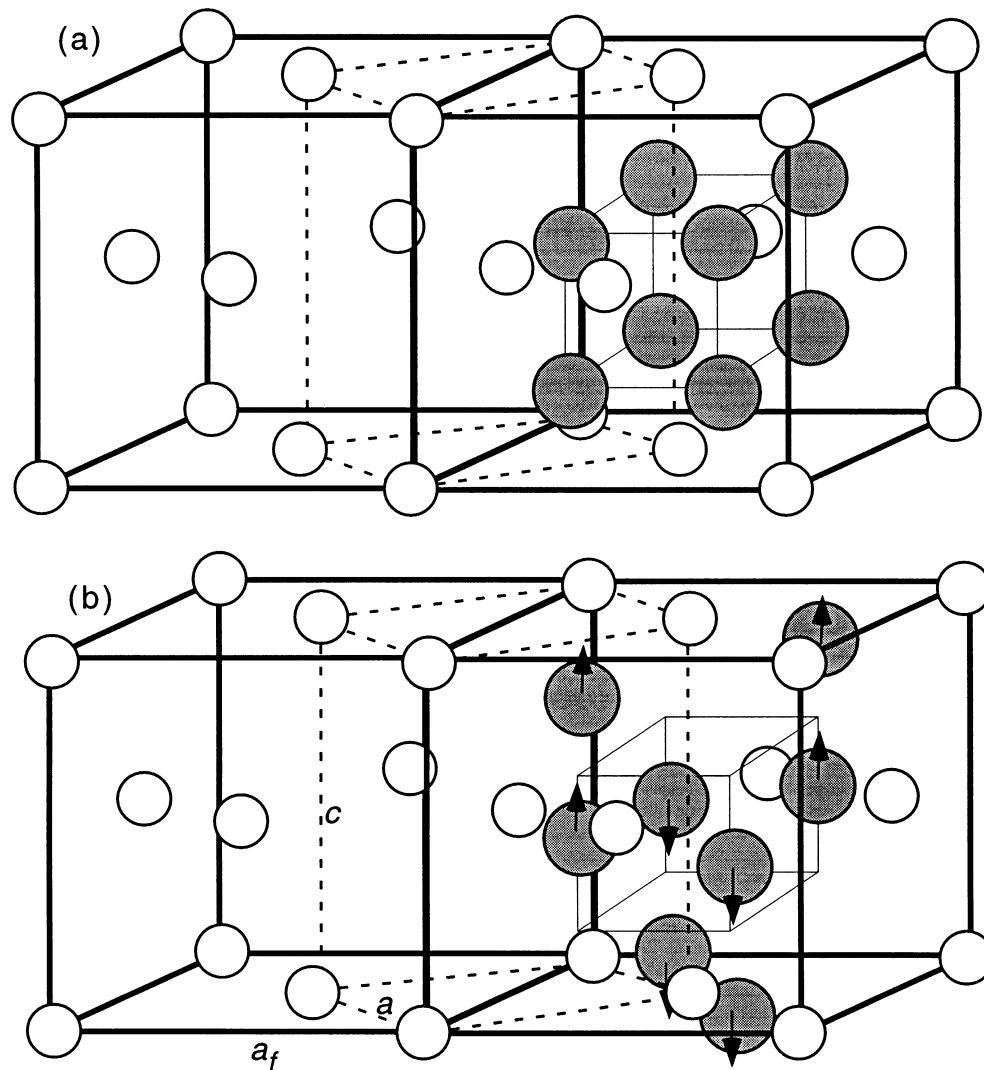


Fig. 3. Spatial relations between (a) cubic and (b) tetragonal  $r''$  cell of  $(\text{Ce,Zr})\text{-O}_2$ . The small circles are the cations and the solid circles are the anions.  $a_f$  is the unit cell dimension of the cubic cell,  $a$  and  $c$  are the parameters for the tetragonal cell.

responsible for the enhancement of oxygen storage observed over these catalysts [41].

Using the above diffusion coefficients, it is possible to estimate the free mean path ( $\lambda$ ) of  $\text{O}^{2-}$  in Ceria and  $\text{CeO}_2\text{-ZrO}_2$  crystallites using the relation  $\lambda = (Dt)^{0.5}$  where  $D$  ( $\text{cm}^2 \text{s}^{-1}$ ) is the diffusion coefficient and  $t$  (s) is time. The values for various frequencies are reported in Fig. 5. The data show that, for a specific oscillation frequency, there is a temperature of *threshold*, dependent on the composition and the size of the crystallites, beyond which the bulk oxygen ions are involved. For example at 673 K, for the time scale of 1 s, the oxygen-ion free mean path in ceria is of the order of 1 nm, whereas in the  $\text{CeO}_2\text{-ZrO}_2$  mixed oxides it lies in the range 5–15 nm. Since the value of mean crystal size is around 8 nm for a surface area of  $100 \text{ m}^2 \text{ g}^{-1}$ , participation of bulk oxygen ions in the CO redox process is expected only for ceria–zirconia. The timescale of bulk diffusion for ceria in the cycling experi-

ments with a frequency of 1 Hz is therefore too great to be of importance. This is also in agreement with what was found by Nibbelke et al. [56], who did not consider bulk oxygen diffusion when modeling CO oxidation under cycling conditions, even for a frequency of 0.25 Hz (i.e. a time scale of 4 s). Conversely, bulk oxygen can participate in the redox process with ceria–zirconia catalysts, even at 673 K, and with a time scale of one second, depending on crystallite dimensions.

## 5. The $\text{CeO}_2\text{-SiO}_2$ system

Several studies have been carried out on the  $\text{CeO}_2\text{-SiO}_2$  system, especially with ceria supported on silica [57–60]. These studies were mainly focused on the behavior of supported ceria and its interaction with the support. A few studies were also concentrated on the thermal stabilization

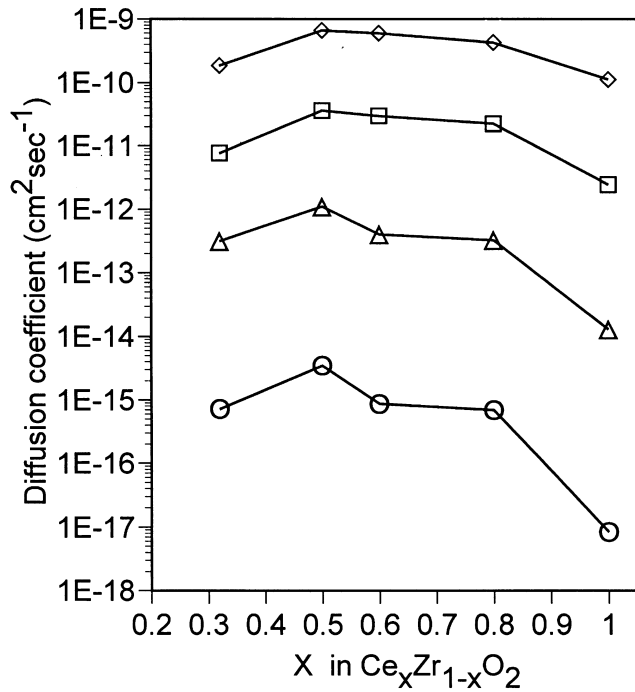


Fig. 4. Calculated diffusion coefficients versus composition at various temperatures: (○) 573 K, (△) 773 K, (□) 973 K, (◇) 1173 K.

of ceria with silicon compounds [61,62]. We have also recently investigated the structural/morphological and redox properties of silica-doped ceria under reducing and oxidizing conditions [28]. The presence of silica strongly modifies the textural properties of ceria and its thermal behavior. Fig. 6 shows that by increasing the amount of silica an increase of the surface area is observed; in addition surface area drop at high temperature is delayed by more than 200 K compared to pure ceria. Silica does not form solid solutions with ceria and the material consists mainly of large separate domains of the two oxides. Under particular redox conditions (treating the sample with a reduction/oxidation cycle), in the presence of silica, the reducibility of ceria is deeply affected and reduction degrees as large as 80% (based on the process  $CeO_2/CeO_{2-x}$ ) can be obtained, which compares favorably with a value of ca. 50% for pure ceria. This occurs in a fashion similar to that observed by doping with  $ZrO_2$ . However, the origin of this promotion does not depend on structural perturbation in the lattice of ceria induced by the dopant, but on the formation of a new phase/compound which then rearranges stabilizing small ceria crystallites.

Evidence for formation of  $Ce_{9.33}(SiO_4)_6O_2$  under reducing conditions were obtained by HRTEM and XRD. The

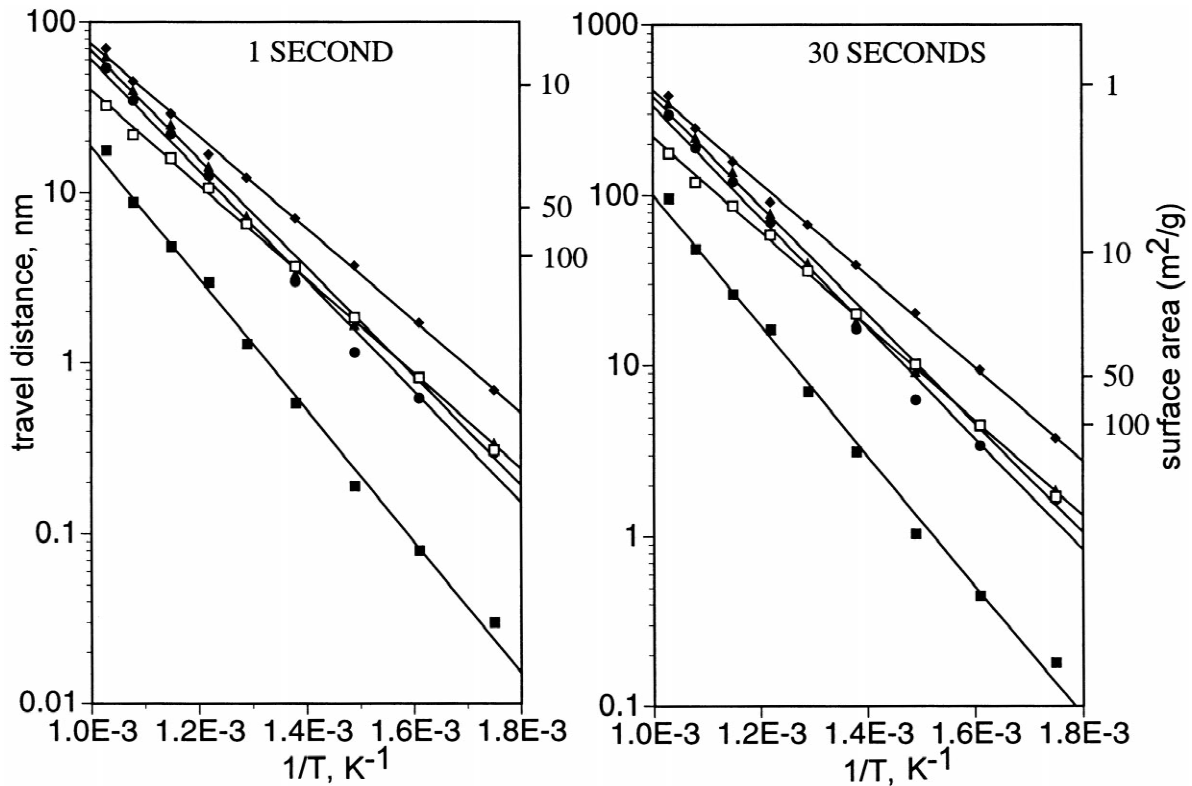


Fig. 5. Calculated travel distance of oxygen ( $\lambda$ ) in time scale of 1 and 30 s against temperature: (■)  $CeO_2$ , (▲)  $Ce_{0.8}Zr_{0.2}O_2$ , (●)  $Ce_{0.68}Zr_{0.32}O_2$ , (◆)  $Ce_{0.5}Zr_{0.5}O_2$ , (▼)  $Ce_{0.15}Zr_{0.85}O_2$ .

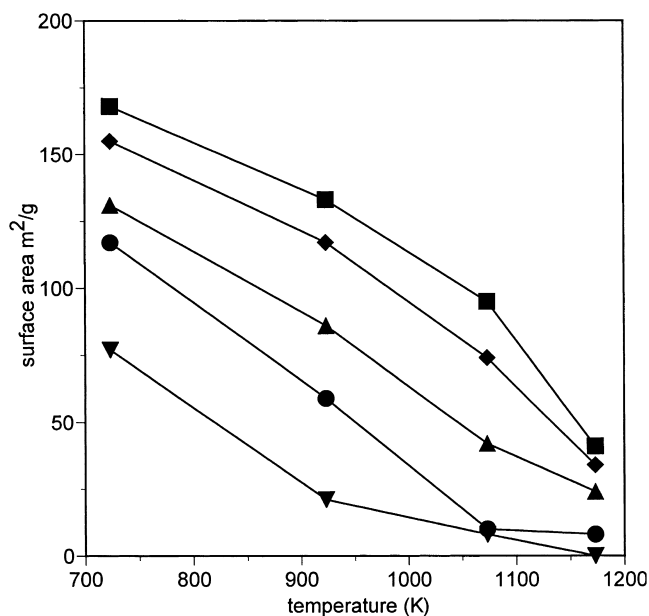
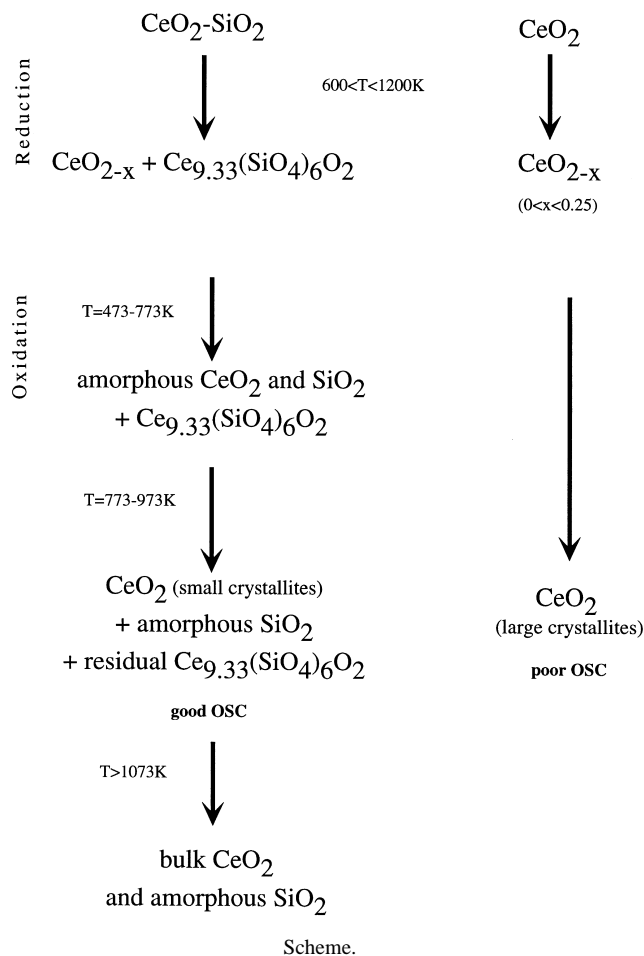


Fig. 6. Surface area against calcination temperature in  $\text{CeO}_2\text{-SiO}_2$  composites with various Si content (% wt): (▼) 0.02, (●) 0.33, (▲) 1.18, (◆) 3.17, (■) 5.49.



formation of this phase allows to overcome the limitations in the reduction of ceria imposed by thermodynamics and almost 80% of cerium formally shifts to the +3 oxidation state in the form of cerium silicate. This phase on reoxidation decomposes giving amorphous silica and small ceria crystallites which are much more reactive toward reduction and oxidation. Nanocrystalline ceria has in fact a lower energy of reduction compared to bulk ceria, and is responsible for a higher defect population [63,64]. Following further redox cycles, Ce–Si phase and nanocrystalline ceria are alternately reformed as evidenced by TPR and XRD measurements. As a comparison, the transformation of the materials are summarized in the scheme. It was shown that whereas fresh ceria has a better OSC than ceria–silica (18  $\mu\text{mol}$  of  $\text{O}_2$  released per gram compared to 14 measured under pulse conditions [28]) the situation is reversed after a redox cycle, where ceria–silica has a superior OSC (5 vs. 1  $\mu\text{mol}$ ).

## 6. Conclusions

In summary the doping of ceria with silica and especially with zirconia induces important structural transformations which depend on the amount of dopant and on the thermal history of the sample. In the case of zirconia, transport properties are believed to be a key factor in the enhancement of the oxygen storage/release capacity under catalytic conditions while with silica the stabilization of small ceria crystallites under catalytic conditions is the factor responsible for the enhancement of activity. The significant result is that doping under certain conditions increases the amount of available oxygen from ceria and is responsible for the increase of OSC and catalytic activity. This can be of benefit also in other catalytic systems where oxygen from support is needed, like catalytic oxidation of large molecules or catalytic oxidation under anaerobic redox conditions [65,66].

## References

- [1] A. Trovarelli, C. de Leitenburg, M. Boaro, G. Dolcetti, *Catal. Today* 50 (1999) 353, and Refs. therein.
- [2] S. Bernal, J. Kaspar, A. Trovarelli (Eds.), *Recent progress in catalysis by ceria and related compounds*, in: *Catal. Today*, Vol. 50(2), 1999, pp. 173–443.
- [3] A. Trovarelli, *Catal. Rev. Sci. Eng.* 38 (1996) 439.
- [4] A. Trovarelli, *Commun. Inorg. Chem.* 20 (1999) 263.
- [5] A. Trovarelli, C. de Leitenburg, G. Dolcetti, *CHEMTECH* 27 (1997) 32.
- [6] J. Kaspar, P. Fornasiero, M. Graziani, *Catal. Today* 50 (1999) 285.
- [7] K.C. Taylor, in: J.R. Anderson, M. Boudart (Eds.), *Catalysis, Science and Technology*, Springer, Berlin, 1984, p. 119.
- [8] M. Ricken, J. Nölting, I. Riess, *J. Solid State Chem.* 54 (1984) 89.
- [9] J. Zhang, Z.C. Kang, L. Eyring, *J. Alloys Comp.* 192 (1993) 57.
- [10] S.J. Schmiege, D.N. Belton, *Appl. Catal. B: Environ.* 6 (1995) 127.

- [11] V. Perrichon, A. Laachir, S. Abournadasse, O. Touret, G. Blanchard, *Appl. Catal. A: General* 129 (1995) 69.
- [12] D. Terribile, A. Trovarelli, J. Llorca, C. de Leitenburg, G. Dolcetti, *J. Catal.* 178 (1998) 299.
- [13] A. Martinez-Arias, M. Fernandez-Garcia, L.N. Salamanca, R.X. Valenzuela, J.C. Conesa, J. Soria, *J. Phys. Chem. B* 104 (2000) 4038.
- [14] P. Fornasiero, R. Di Monte, G. Ranga Rao, J. Kaspar, S. Meriani, A. Trovarelli, M. Graziani, *J. Catal.* 151 (1995) 168.
- [15] B.K. Cho, *J. Catal.* 131 (1991) 74.
- [16] P. Vidmar, P. Fornasiero, J. Kaspar, G. Gubitosa, M. Graziani, *J. Catal.* 171 (1997) 160.
- [17] A.R. West, in: *Solid State Chemistry and its Applications*, Wiley, New York, 1984.
- [18] P. Shuk, M. Greenblatt, M. Croft, *Chem. Mater.* 11 (1999) 473.
- [19] C.K. Narula, L.P. Haack, W. Chun, H.-W. Jen, G.W. Graham, *J. Phys. Chem. B* 103 (1999) 3634.
- [20] F. Zamar, A. Trovarelli, C. de Leitenburg, G. Dolcetti, *Stud. Surf. Sci. Catal.* 101 (1996) 1283.
- [21] S. Bernal, G. Blanco, M.A. Cauqui, P. Corchado, J.M. Pintado, J.M. Rodriguez-Izquierdo, *Chem. Commun.* (1997) 1545.
- [22] A.D. Logan, M. Shelef, *J. Mater. Res.* 9 (1994) 468.
- [23] R.D. Shannon, C.T. Prewitt, *Acta Crystallogr. B* 25 (1969) 925.
- [24] M. Yashima, H. Arashi, M. Kakihana, M. Yoshimura, *J. Am. Ceram. Soc.* 77 (1994) 1067.
- [25] Y. Zhang, A. Andersson, M. Muhammed, *Appl. Catal. B: Environ.* 6 (1995) 325.
- [26] C. Lammonier, A. Bennani, A. D'Huysser, A. Aboukaïs, G. Wrobel, *J. Chem. Soc. Faraday Trans.* 92 (1996) 131.
- [27] S. Imamura, M. Shono, N. Okamoto, A. Haneda, S. Ishida, *Appl. Catal. A: General* 142 (1996) 279.
- [28] E. Rocchini, A. Trovarelli, J. Llorca, G.W. Graham, H. Weber, M. Maciejewski, A. Baiker, *J. Catal.* 194 (2000) 461.
- [29] M. Ozawa, M. Kimura, A. Isogai, *J. Alloys Comp.* 193 (1993) 73.
- [30] T. Murota, T. Hasegawa, S. Aozasa, H. Matsui, M. Motoyama, *J. Alloys Comp.* 193 (1993) 298.
- [31] C.E. Hori, H. Permana, K.Y.S. Ng, A. Brenner, K. More, K.M. Rahmoeller, D. Belton, *Appl. Catal. B* 16 (1998) 105.
- [32] H. Vidal, J. Kaspar, M. Pijolat, G. Colon, S. Bernal, A. Cordon, V. Perrichon, F. Fally, *Appl. Catal. B: Environ.* 27 (2000) 49.
- [33] Y. Madier, C. Descorme, A.M. Le Govic, D. Duprez, *J. Phys. Chem. B* 103 (1999) 10999.
- [34] H.-W. Jen, G.W. Graham, W. Chun, R.W. McCabe, J.-P. Cuif, S.E. Deutsch, O. Touret, *Catal. Today* 50 (1999) 309.
- [35] J.R. Gonzales-Velasco, M.A. Gutierrez-Ortiz, J.-L. Marc, J.A. Botas, M. Pilar Gonzales-Marcos, G. Blanchard, *Appl. Catal. B: Environ.* 25 (2000) 19.
- [36] M. Ozawa, C.-K. Loong, *Catal. Today* 50 (1999) 329.
- [37] C. Bozo, N. Guilhaume, E. Garbowski, M. Primet, *Catal. Today* 59 (2000) 33.
- [38] C. de Leitenburg, D. Goi, A. Primavera, A. Trovarelli, G. Dolcetti, *Appl. Catal. B: Environ.* 11 (1996) L29.
- [39] F. Zamar, A. Trovarelli, C. de Leitenburg, G. Dolcetti, *J. Chem. Soc. Chem. Commun.* (1995) 965.
- [40] D. Terribile, A. Trovarelli, C. de Leitenburg, A. Primavera, G. Dolcetti, *Catal. Today* 47 (1999) 133.
- [41] M. Boaro, C. de Leitenburg, G. Dolcetti, A. Trovarelli, *J. Catal.* 193 (2000) 338.
- [42] M. Yashima, K. Morimoto, N. Ishizawa, M. Yoshimura, *J. Am. Ceram. Soc.* 76 (1993) 2865.
- [43] M. Yashima, S. Sasaki, M. Kakihana, Y. Yamaguchi, H. Arashi, M. Yoshimura, *Acta Crystallogr. B* 50 (1994) 663.
- [44] S. Rossignol, F. Gerard, D. Duprez, *J. Mater. Chem.* 9 (1999) 1615.
- [45] G. Balducci, P. Fornasiero, R. Di Monte, J. Kaspar, S. Meriani, M. Graziani, *Catal. Lett.* 33 (1995) 193.
- [46] D. Terribile, A. Trovarelli, J. Llorca, C. de Leitenburg, G. Dolcetti, *Catal. Today* 43 (1998) 79.
- [47] T. Masui, K. Fujiwara, Y. Peng, T. Sakata, K. Machida, H. Mori, G. Adachi, *J. Alloys Comp.* 269 (1998) 116.
- [48] T. Ozaki, T. Masui, K. Machida, G. Adachi, T. Sakata, H. Mori, *Chem. Mater.* 12 (2000) 643.
- [49] A. Trovarelli, F. Zamar, J. Llorca, C. de Leitenburg, G. Dolcetti, J. Kiss, *J. Catal.* 169 (1997) 490.
- [50] S. Enzo, R. Frattini, F. Delogu, A. Primavera, A. Trovarelli, *J. Mater. Res.* 15 (2000) 1538.
- [51] P. Fornasiero, G. Balducci, R. Di Monte, J. Kaspar, V. Sergo, G. Gubitosa, A. Ferrero, M. Graziani, *J. Catal.* 164 (1996) 173.
- [52] W. Stichert, F. Schuth, *Chem. Mater.* 10 (1998) 2020.
- [53] M. Yashima, S. Sasaki, Y. Yamaguchi, M. Kakihana, M. Yoshimura, T. Mori, *Appl. Phys. Lett.* 72 (1998) 182.
- [54] T. Omata, H. Kishimoto, S. Otsuka-Yao-Matsuo, N. Ohtori, N. Umesaki, *J. Solid State Chem.* 147 (1999) 573.
- [55] G. Chiodelli, G. Flor, M. Scagliotti, *Solid State Ionics* 91 (1996) 109.
- [56] R.H. Nibbelke, A.J.L. Nievergeld, J.H.B.J. Hoebink, G.B. Marin, *Appl. Catal. B: Environ.* 19 (1998) 245.
- [57] L. Kepinski, M. Wolcyrz, *J. Solid State Chem.* 131 (1997) 121.
- [58] M. Haneda, T. Mizushima, N. Kakuta, A. Ueno, *Bull. Chem. Soc. Jpn.* 67 (1994) 2617.
- [59] R. Craciun, *Solid State Ionics* 110 (1998) 83.
- [60] A. Bensalem, F. Bozon-Verduraz, M. Delamar, G. Bugli, *Appl. Catal. A: General* 121 (1995) 81.
- [61] G.N. Sauvion, J. Caillod, C. Gourlaouen, *US Patent* 4.949.685 (1990).
- [62] L. Bonneau, T. Chopin, O. Touret, *US Patent* 5.529.969 (1996).
- [63] J.H. Hwang, T.O. Mason, *Z. Phys. Chem.* 207 (1998) 21.
- [64] F. Giordano, A. Trovarelli, C. de Leitenburg, M. Giona, *J. Catal.* 193 (2000) 273.
- [65] L. Oliviero, J. Barbier Jr., S. Labruquere, D. Duprez, *Catal. Lett.* 60 (1999) 15.
- [66] K. Otsuka, Y. Wang, M. Nakamura, *Appl. Catal. A: General* 183 (1999) 317.